

SUPPLEMENTAL FIGURE LEGENDS

Figure S1. A) Immunofluorescence for Yap1 localization in confluent HaCaT cells following siRNA transfection of selected kinase hits. B) Western Blot for Yap S127 phosphorylation, and total Yap in 293T cells four days following siRNA transfection of selected kinase hits

Figure S2. A) Mitogen activated kinase pathway siRNA mini-screen using the STBS-luciferase reporter in 293T cells compared to scrambled control (CTR). B) Selective JNK small molecule screen using the STBS-luciferase reporter in 293T cells. Schematic demonstrates where the inhibitors function. Fold changes calculated are compared to untreated controls.

Figure S3. A) Knockdown of LKB1 using multiple different siRNA oligos increases STBS-luciferase reporter activity in 293T cells. B) Knockdown of LKB1 reproducibly increases STBS-luciferase reporter activity across various cell lines. C) Knockdown of LKB1 reproducibly decreases Yap S127 phosphorylation across various cell lines by western blot analysis. D) Knockdown of LKB1 in DLD1 cells promotes Yap1 nuclear localization at confluent cell densities. E) qPCR validation of LKB1 and Yap siRNA knockdown in 293T cells. F) LKB1 activation in W4 cells repressed TEAD-reporter activation. Error bars represent \pm SD from triplicate samples.

Figure S4. A) Representative image of Livers isolated from p53, p53/Lkb1fl/fl mice three months following adenovirus-Cre injection. Average weights of livers were compared to the average body mass. Error bars represent \pm SD from n=4 mice. **, P \leq 0.01. B) Decreased activity of MST1/2 in LKB1 deficient livers. Ratio of cleaved MST1 versus full length MST is

shown for an average from n=4. C) Yap S127 phosphorylation in liver lysates derived from P53^{f/f} and P53/LKB1^{f/f} adeno-Cre infected mice. D) Proliferative status of p53, p53/Lkb1fl/fl liver by Ki67 immunohistochemistry staining. Quantification based on 30 fields of view (FOV) from three mice (10/mouse). E) Expression levels of expressed Lats1, Lats2 and Mob1 for experiments corresponding to Figure 2H. Error bars represent \pm SD.

Figure S5. A) Control immunofluorescence experiment demonstrating that loss of LKB1 in dox-treated/STRAD induced in the W4 cell line has no effect on Yap nuclear localization. B) qPCR validation of knockdown using siRNA's targeting MST1, MST2, LATS1, LATS2. C) Immunofluorescence for Yap localization (green) and cell polarization (red) in doxycycline-untreated W4 cells following knockdown of MST1/2 and Lats1/2. D) Quantification of Yap localization in W4 cells following MST1/2 or Lats1/2 knockdown. 20 fields of view for three independent experiments were quantitated. E) Localization of Yap1 following LKB1-activation and knockdown of MST1 and LATS2 in W4 cells using 2 independent siRNA's. F, G) Immunoprecipitation of overexpressed LKB1, LATS1, and MST1 in 293T cells. Error bars represent \pm SD from triplicate samples.

Figure S6. A) qPCR validation of siRNA knockdown of MARK1 and MARK4 and expression of YAP-target genes, CTGF and CYR61. B) STBS-reporter activation following knockdown of MARKS (1, 3, 4) in MCF-7 and DLD1 cells. C) STBS reporter activity following knockdown of MARK4 and Yap in 293T cells. D) TBS-luciferase activity following MARK knockdown can be repressed by overexpression Mob1, Lats1/2. E) Activation of LKB1 in W4 cells promotes activation of MARKs as measured by Thr215 phosphorylation (MARK1) in the kinase activation loop F) Immunofluorescence for Yap localization (green) and cell polarization (red) in doxycycline-untreated W4 cells following knockdown of MARK4. G) Quantification of Yap localization in W4 cells following MARK knockdown. 20 fields of view for three independent

experiments were quantified. H) Yap localization in W4 cells following LKB1 activation and knockdown of MARK4 using 2 independent siRNA's. Error bars represent \pm SD from triplicate samples.

Figure S7. A) In vitro kinase assay using immunoprecipitated myc-MARK1 and myc-MARK1-KD and recombinant human DLG1 as a substrate. Western blot analysis was performed measuring the degree of serine/threonine phosphorylation on Dlg1 following MARK1 activation. B) Immunofluorescence for Scribble localization (green) in DLD1 cells following LKB1 and MARK siRNA knockdown. C, D) Immunoblot and qPCR for Scribble expression following LKB1 and MARK1 knockdown in MCF7 cells. E) Immunofluorescence and confocal Z-stack for DLG1 localization (green) in MCF7 cells following LKB1 and MARK siRNA knockdown.

Figure S8. A) qPCR validation of scribble knockdown using 3 independent siRNA's. B) siRNA knockdown of scribble in 293T cells induces TEAD-reporter activity C) Immunofluorescence for Yap localization (green) and cell polarization (red) in doxycycline-untreated W4 cells following knockdown of Scribble. D) Quantification of Yap localization in W4 cells following scribble knockdown. 20 fields of view for three independent experiments were quantitated. E) Immunofluorescence for Yap localization following activation of LKB1 and knockdown of scribble using 2 independent siRNA's. F) Immunoprecipitation of overexpressed MARK4 with Scribble, LKB1, MST1, and LATS1. Error bars represent \pm SD from triplicate samples

Figure S9. A) Microarray analysis on three different cell lines following siRNA knockdown of NF2, Lats1/2, and rescue effect following additional knockdown of Yap and Taz. B) A broad spectrum Hippo signature was generated using differentially expressed genes defined as those

with at least 2 fold change in NF2/LATS2 double knockdown cells and a p value smaller than 0.05.

Figure S10. A) Yap immunohistochemistry on murine wild-type pancreas and PDX-cre LKB1fl/fl pancreas. B) Yap1 immunohistochemistry on human SMAD4 juvenile polyposis (JP) intestinal polyp compared to a human LKB1 mutant Peutz-Jeghers (PJ) intestinal polyp.

Figure S11. A) MTS proliferation assay on W4, W4TetOYap, +/- doxycycline cells. B) Soft agar colony formation assay using W4, W4TetOYap, +/- doxycycline 4 weeks after seeding. Quantification of triplicate samples of number and size of W4, W4TetOYap, +/- doxycycline colonies. C) Tumor weights of W4, W4TetOYap, +/- doxycycline after seven weeks. Representative images of nude mice carrying xenografts with W4, W4TetOYap tumors Error bars represent \pm SD from triplicate samples.

Figure S12. A) qPCR validation of shRNA knockdown of LATS2 and activation of Yap-target genes in W4 cells. B) MTS proliferation assay using 2 independent shLATS2 cell line clones (C1, C3). C) Soft agar colony formation assay using W4-shLATS2 cell line clones, C1, C3. D) qPCR of Scribble, and YAP target genes, CYR61 and CTGF following Scribble siRNA knockdown in the presence of LKB1 activation. E) MTS proliferation assay using 2 independent siRNA's against scribble in LKB1-activated W4 cells.

Figure S13. A) Gene expression of Yap1 following 3 days of doxycycline treatment to A549 cells stably expression inducible Yap shRNA hairpin A (A549iYapshRNA). B) Soft agar colony formation assay using A549iYapShRNA, +/- doxycycline 4 weeks after seeding. Quantification of triplicate samples of number and size of W4, W4TetOYap, +/- doxycycline colonies. C) Hematoxilin/Eosin stains on representative murine lungs displaying nodule formation following

intravenous injection of 1×10^6 A549iYapshRNA cells (-/+ doxycycline) for 6 weeks. D, E) Average tumor size and number per mouse following intravenous injection of 1×10^6 A549iYapshRNA cells (-/+ doxycycline) for 6 weeks. F) Panel of LKB1 wild-type lung and LKB1-mutant adenocarcinoma cell lines assessed for Yap-target gene activity, CYR61 and AMOTL2. G-I) Two cell lines that are low in Yap target gene expression were infected with shYAP hairpins (H) and assessed for proliferation using MTS assays (G) and soft agar colony formation assay (I). J) Expression levels of Lkb1 and Yap1 following Ad-cre administration in Lkb1-floxed and Lkb1/Yap1 floxed livers.

SUPPLEMENTARY TABLES

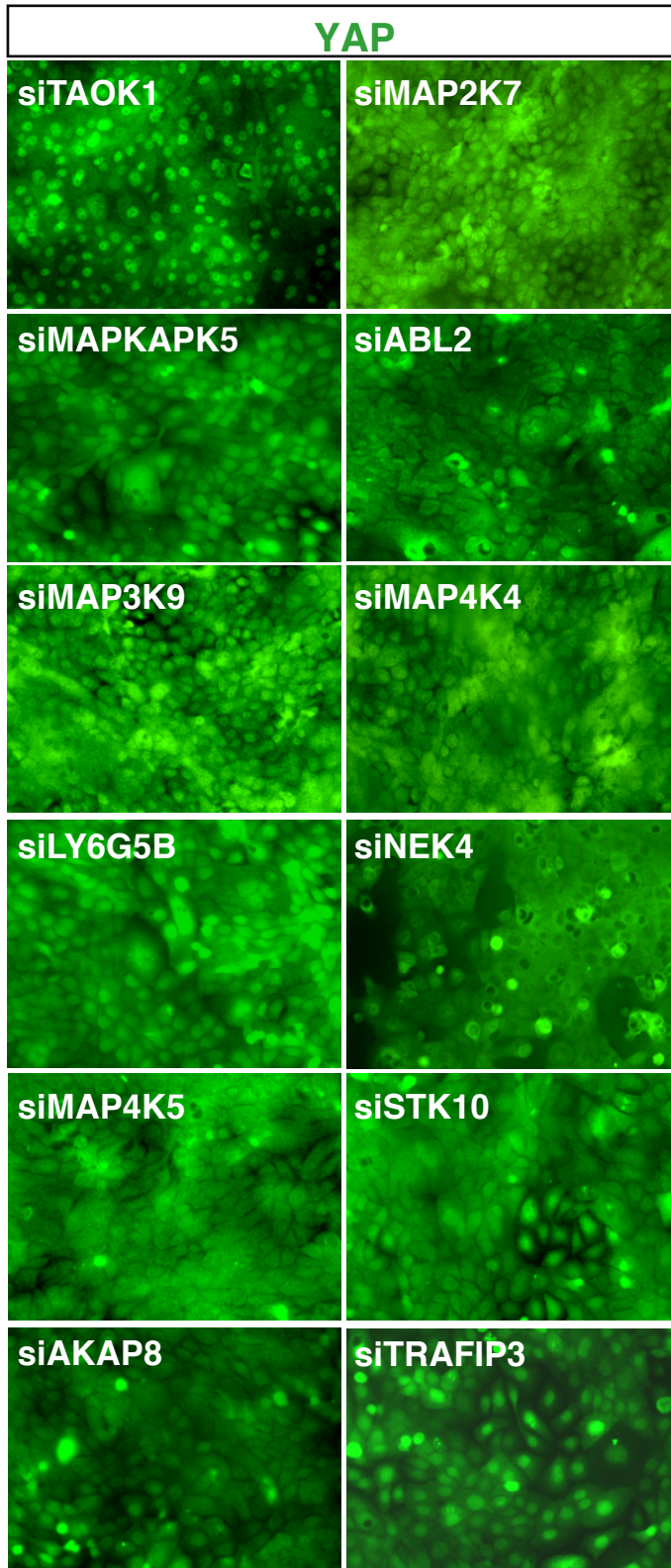
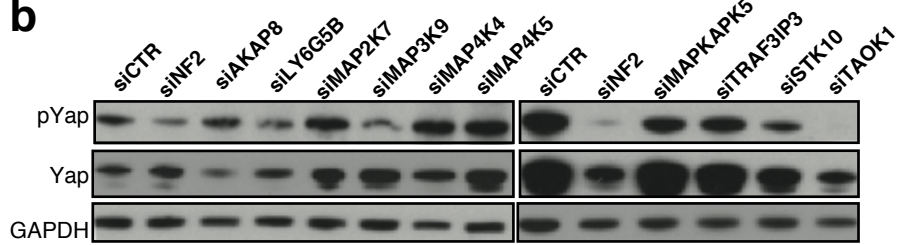
Table S1. Fold changes and Z-scores of the 21 kinases that activated STBS-mCherry in 293T cells. Mean values of triplicate experiments for each oligo (A, B, C) are presented.

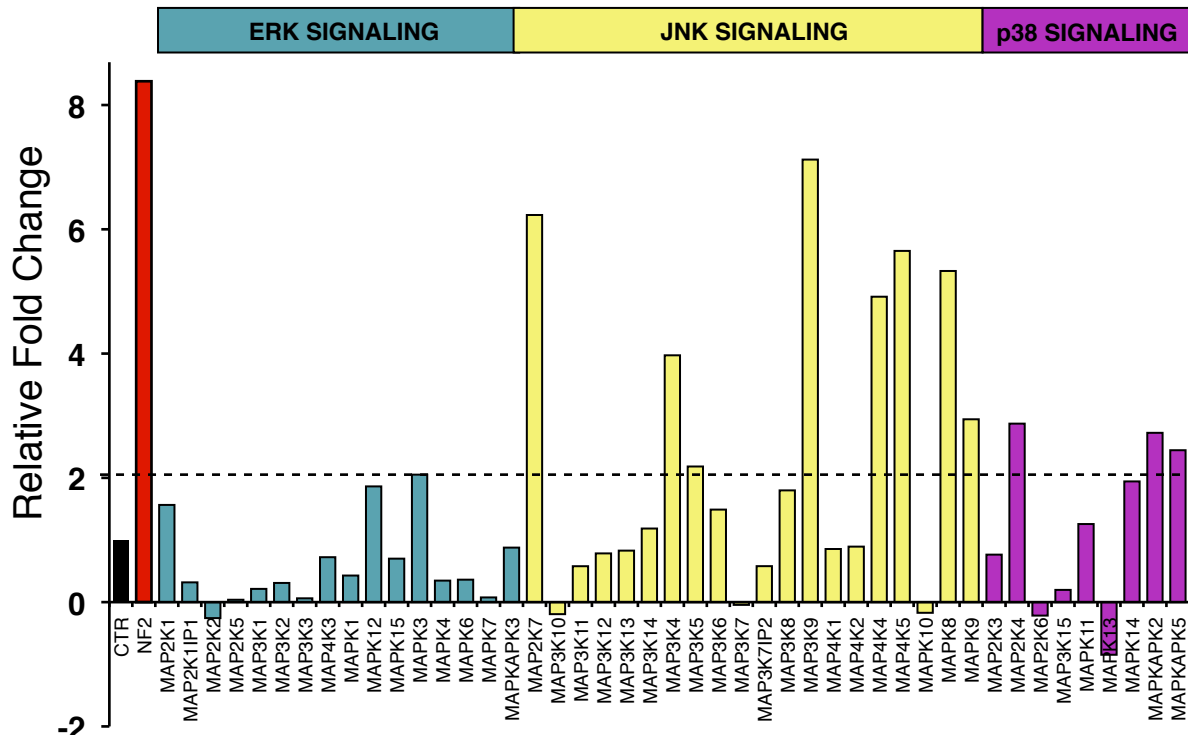
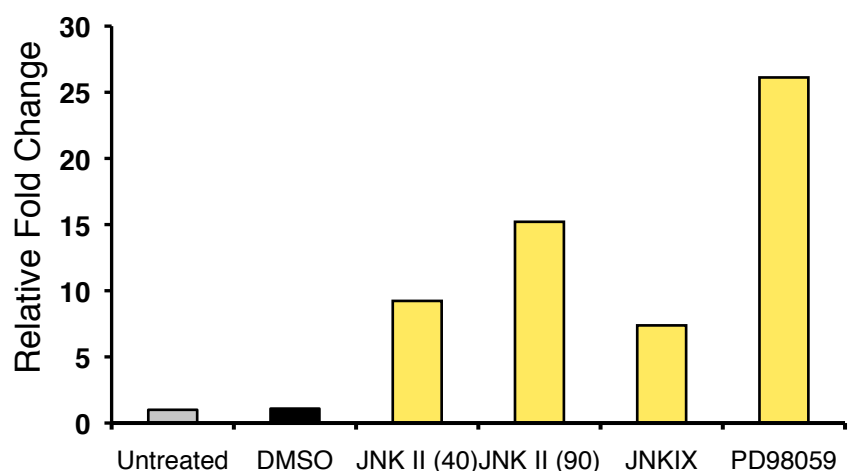
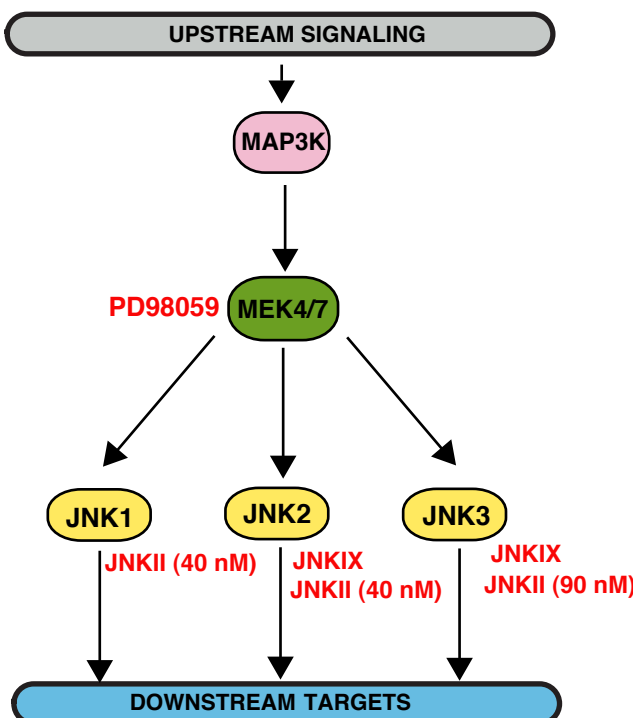
Table S2. Compiled list of STBS-mCherry activation state following knockdown of the MARK and Ephrin family of kinases. Fold changes were compared to the scrambled negative control for each experiment. A, B, C represent different oligonucleotides targeting each kinase.

Type of file: figure

Label: Figure S1, S2, S3, S4, S5, S6, S7, S8, S9, S10, S11, S12, S13

Filename: 44560_0_supp_1865293_mkrpkf_Part1.pdf

a**b****FIGURE S1**

a**b****FIGURE S2**

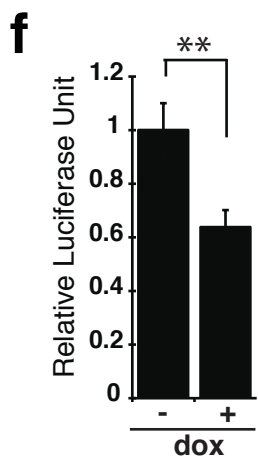
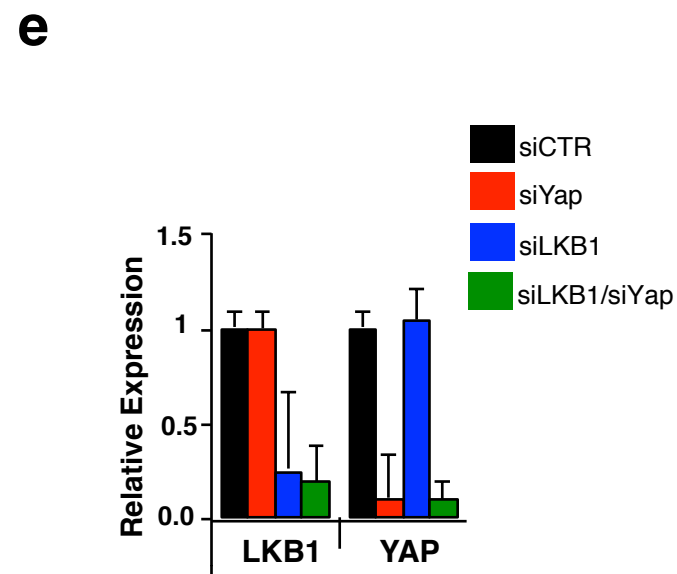
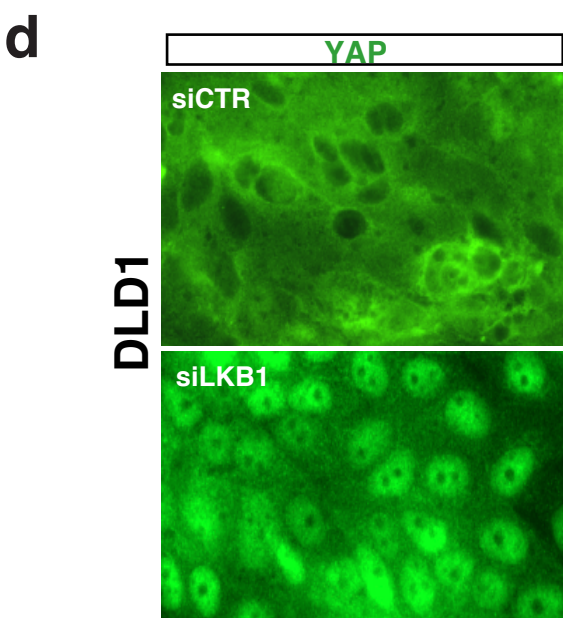
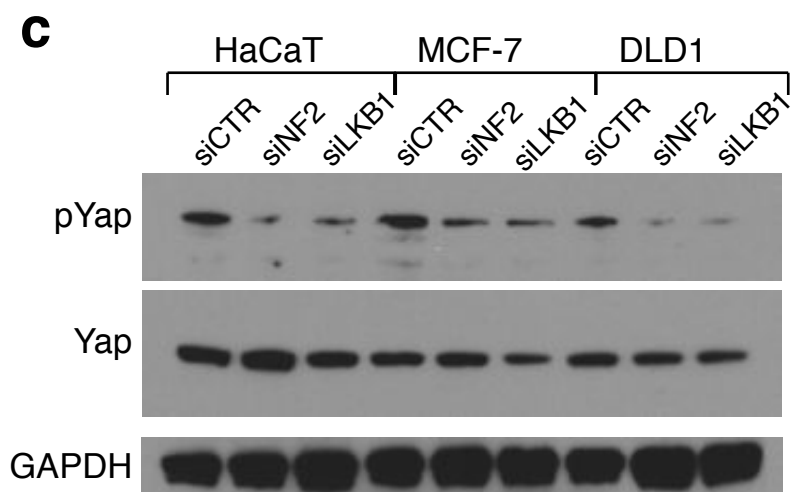
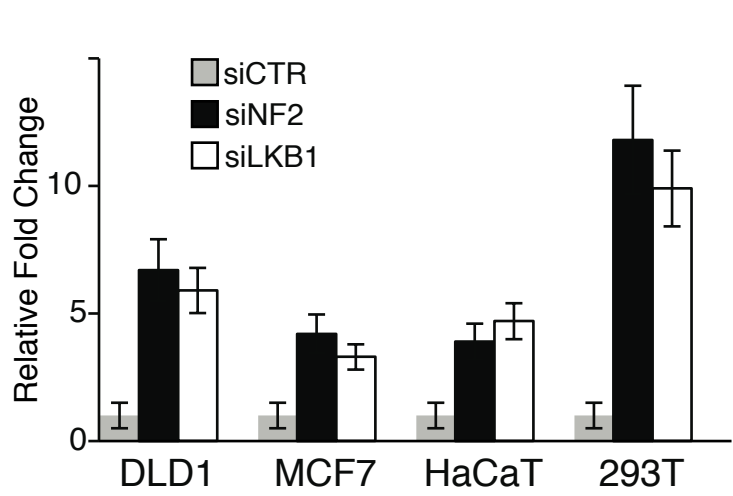
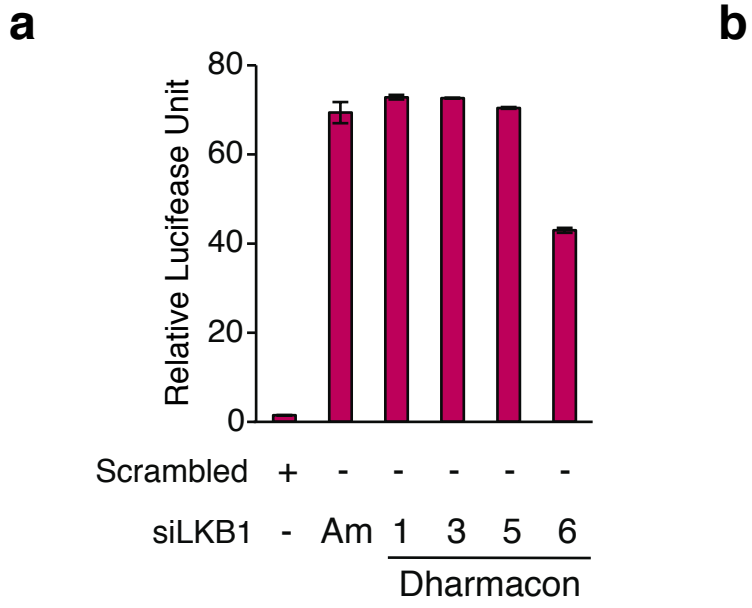
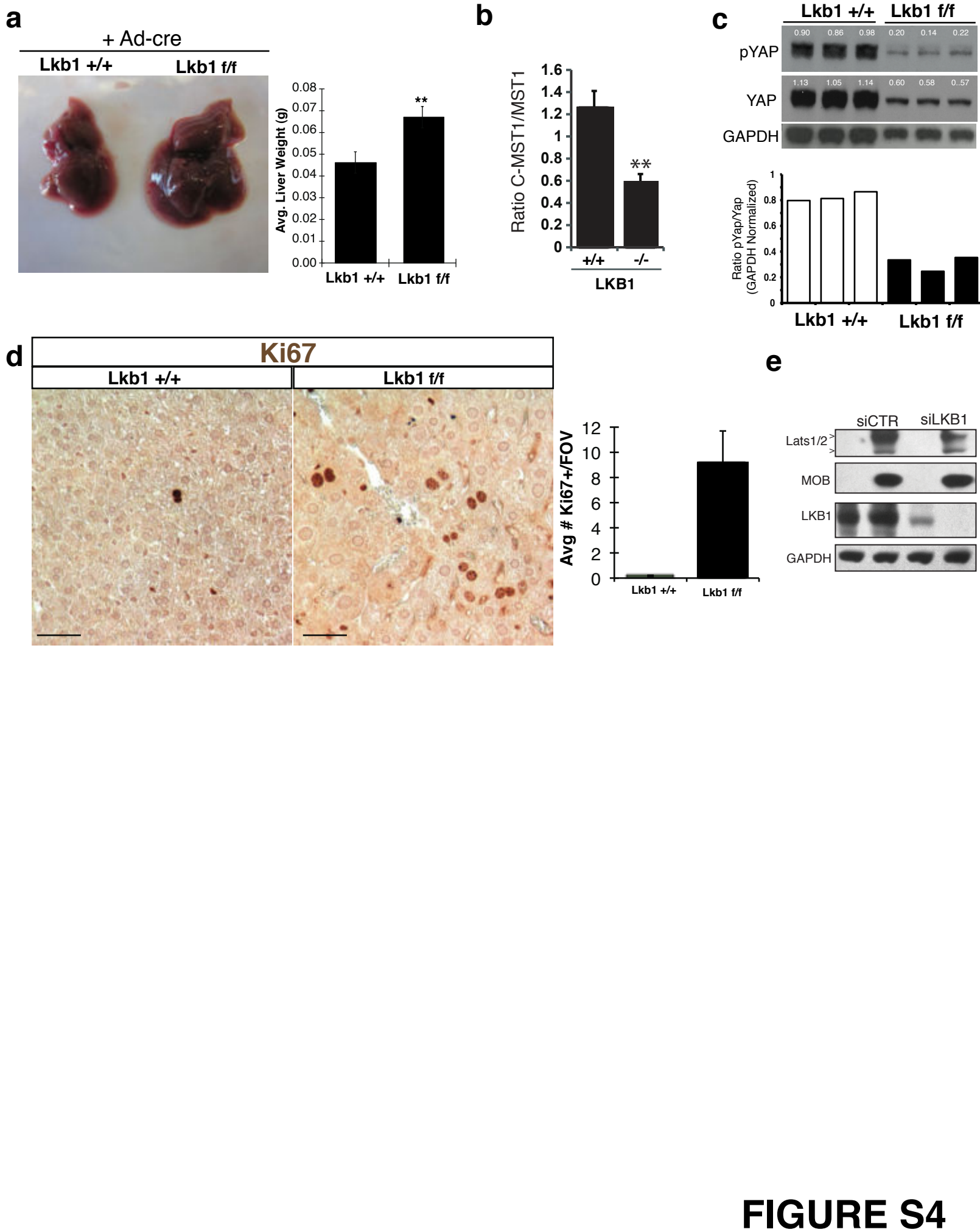


FIGURE S3



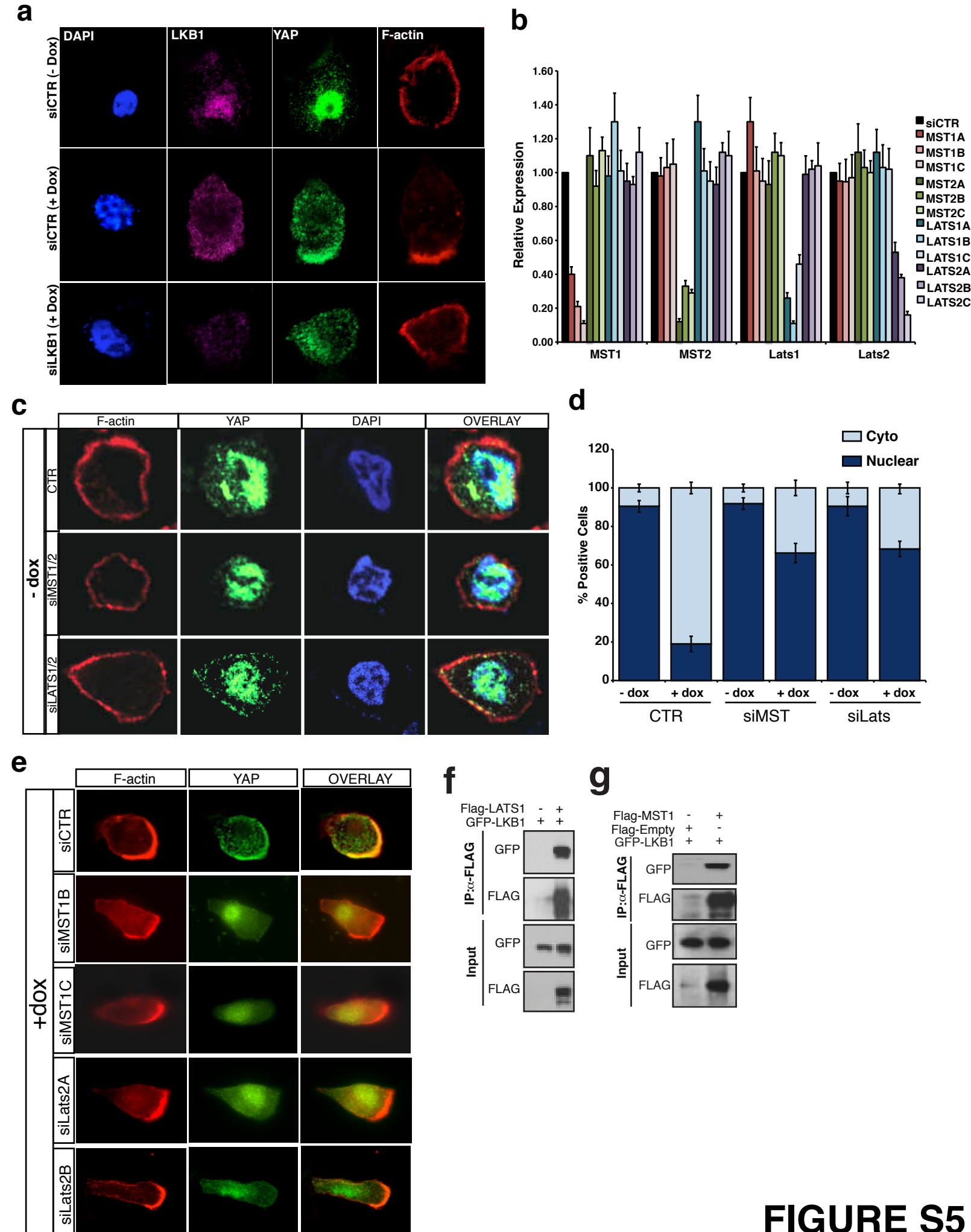
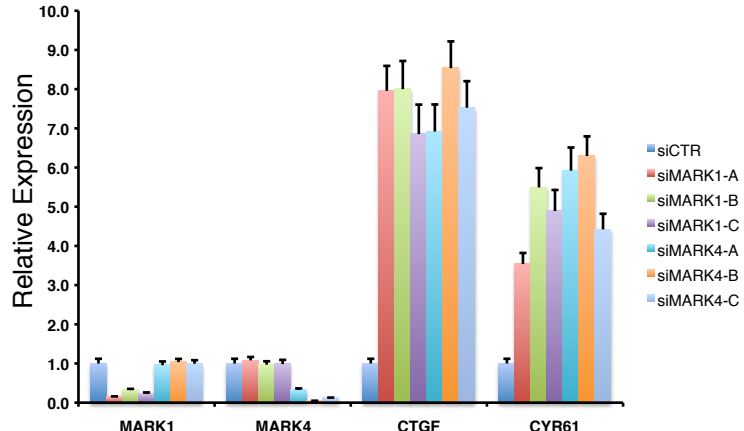
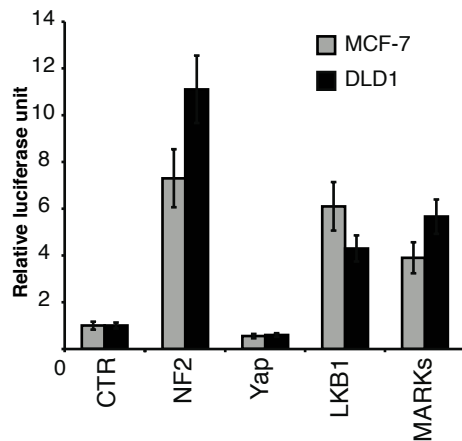
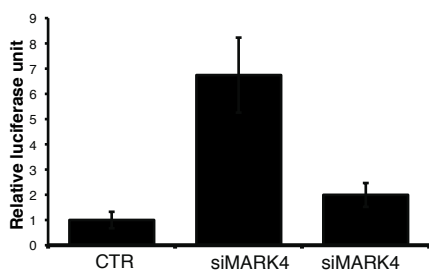
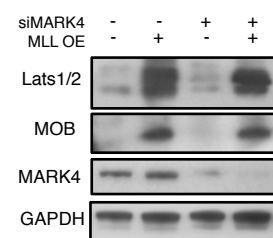
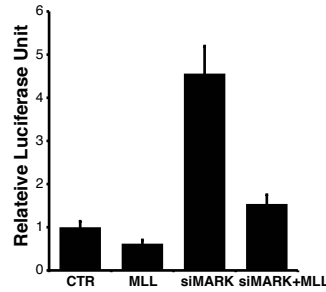
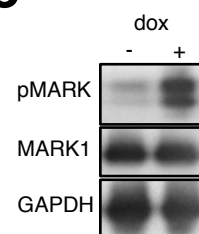
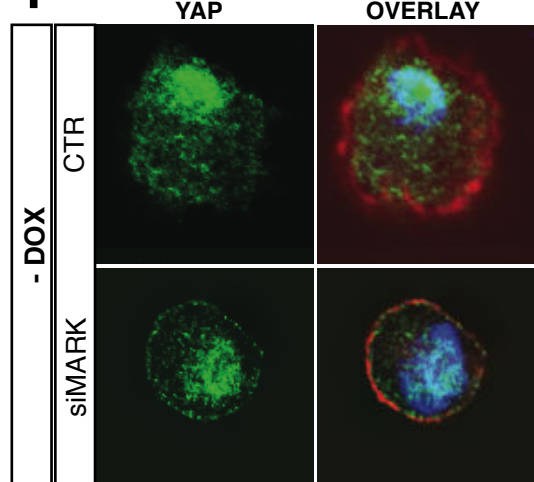
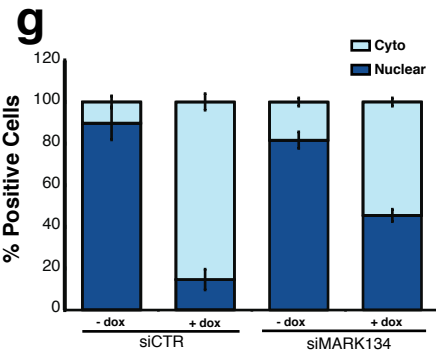
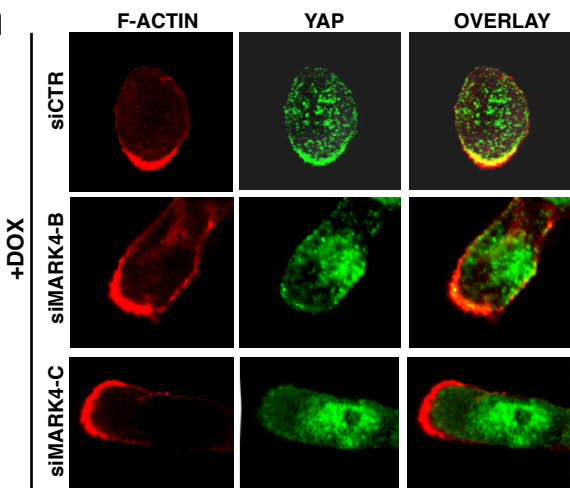
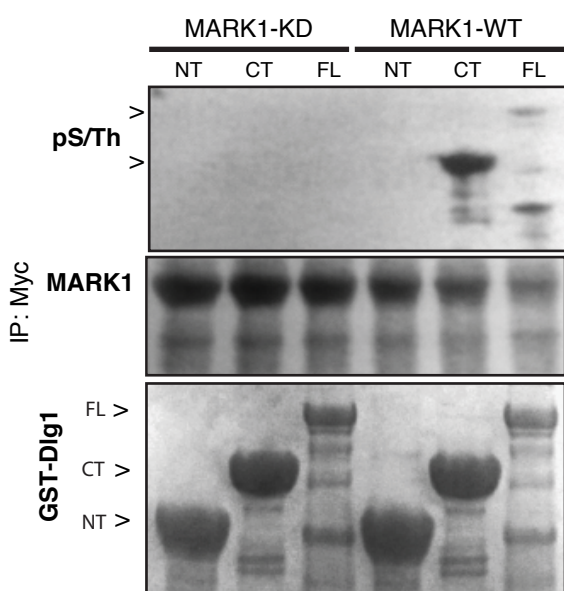
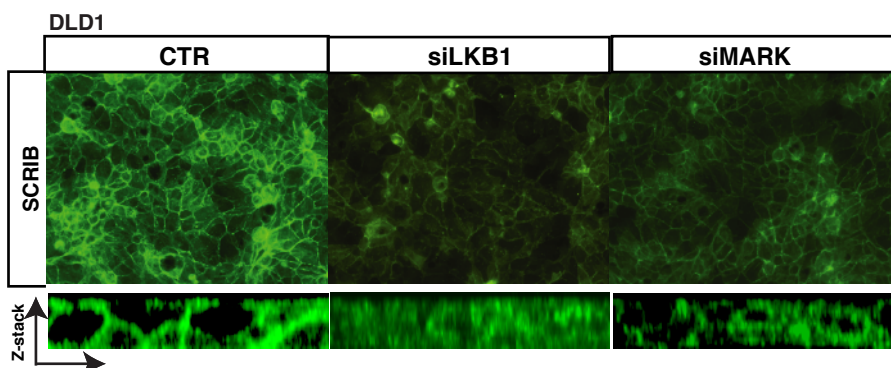
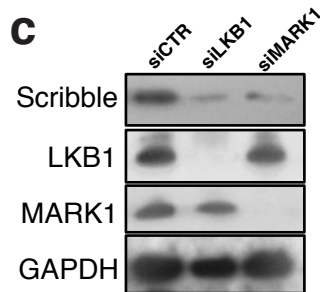
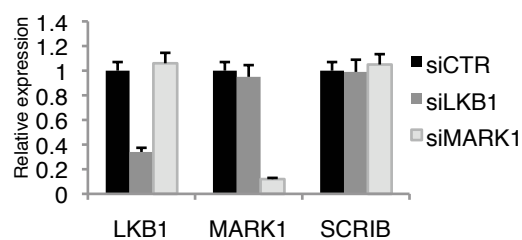
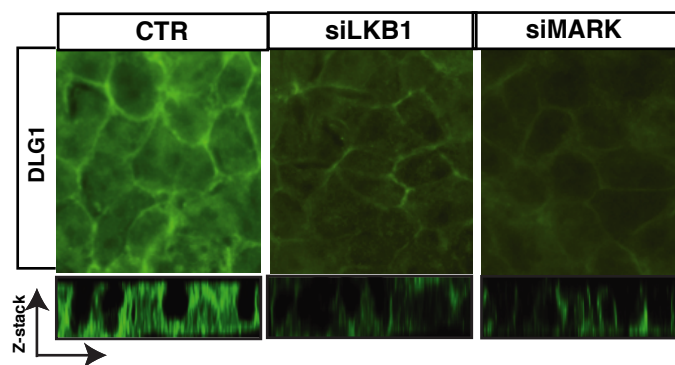


FIGURE S5

a**b****c****d****e****f****g****h****FIGURE S6**

a**b****c****d****e****FIGURE S7**

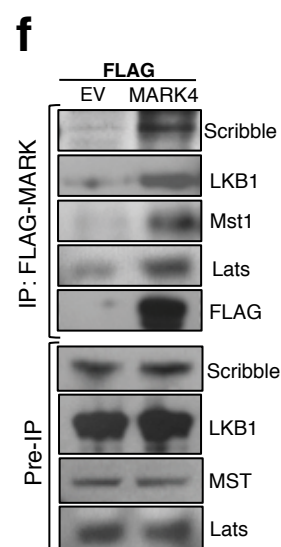
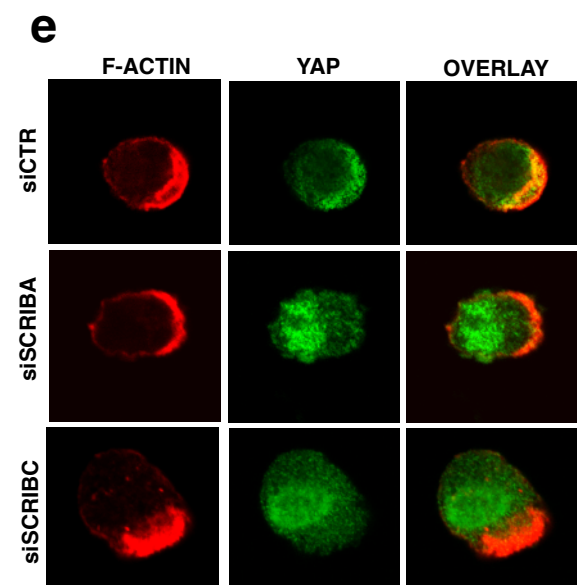
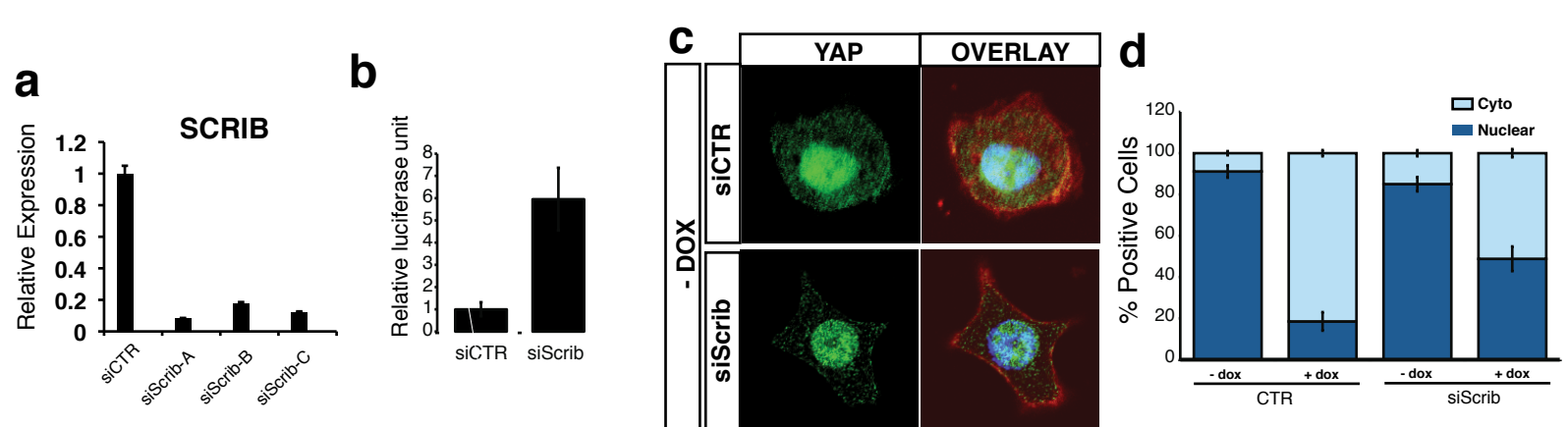
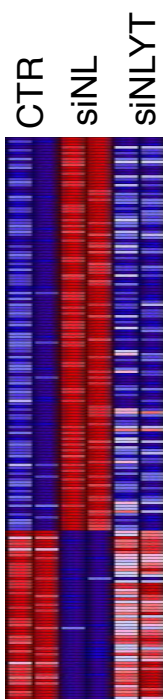
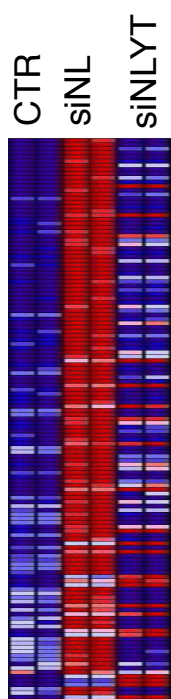


FIGURE S8

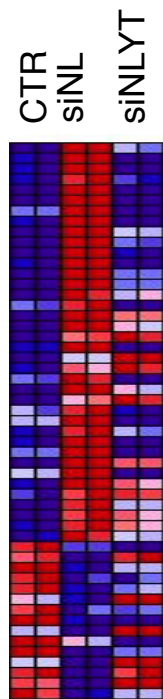
293T



HaCaT



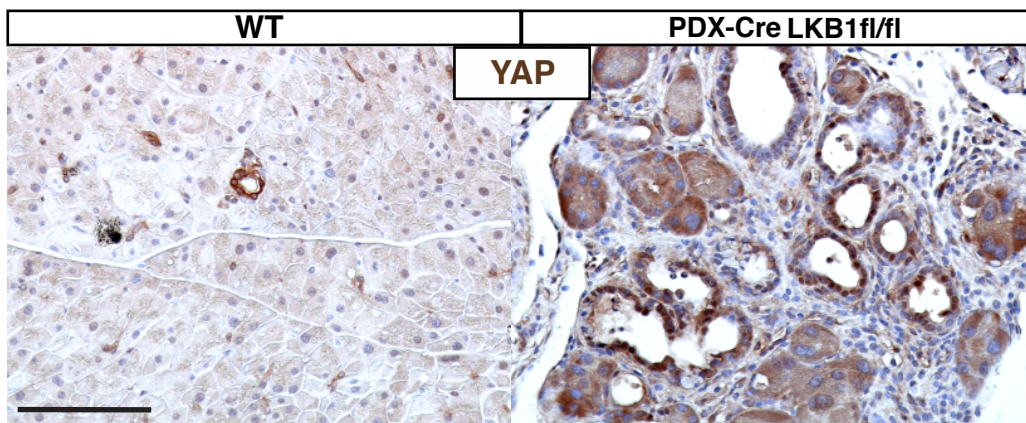
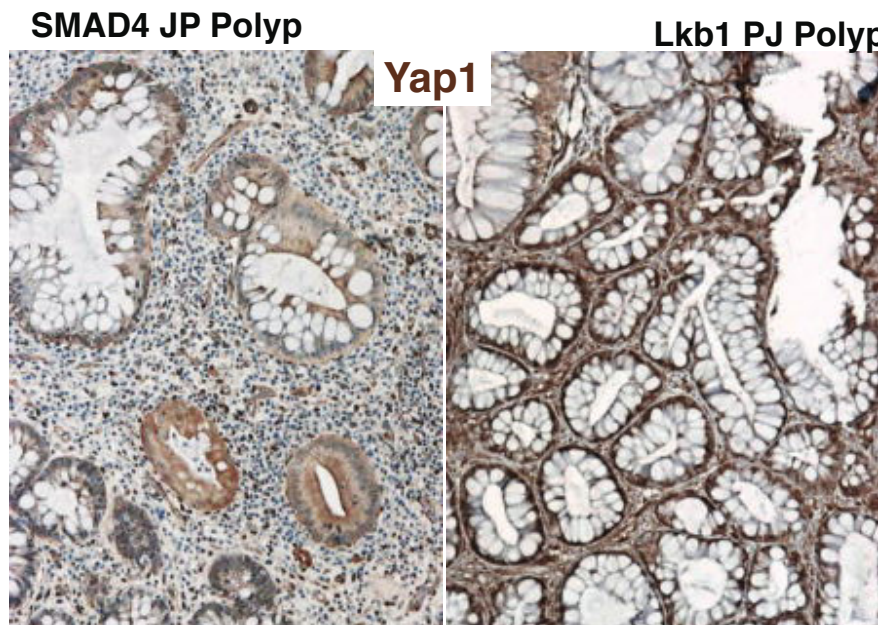
HepG2

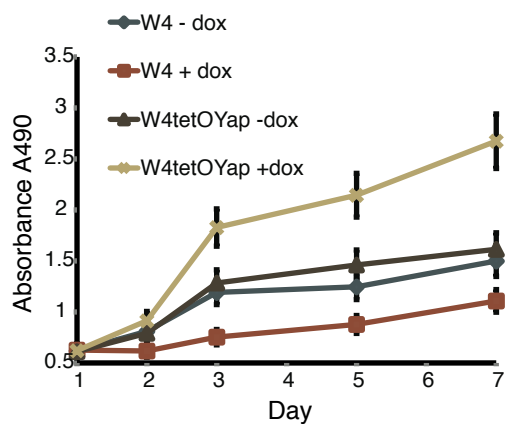
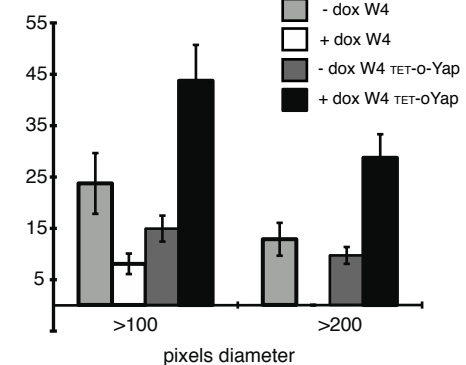
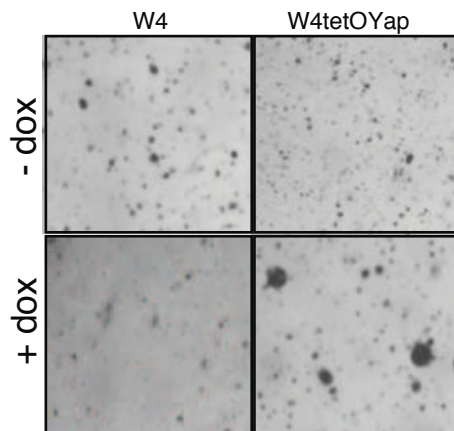
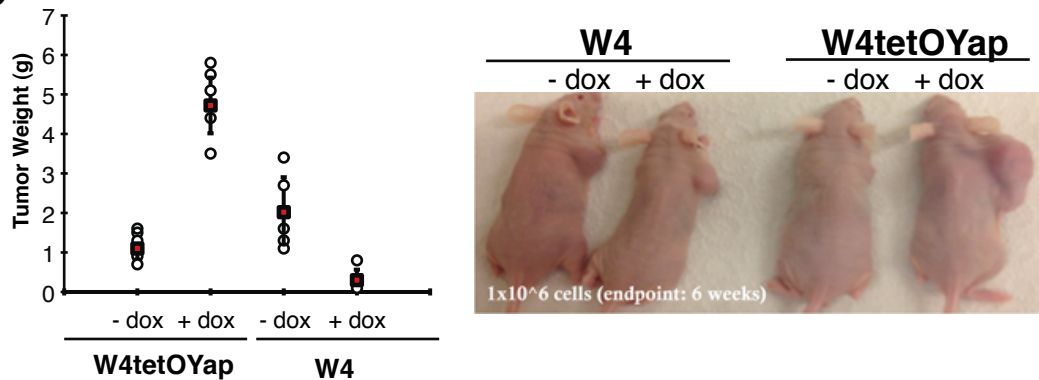


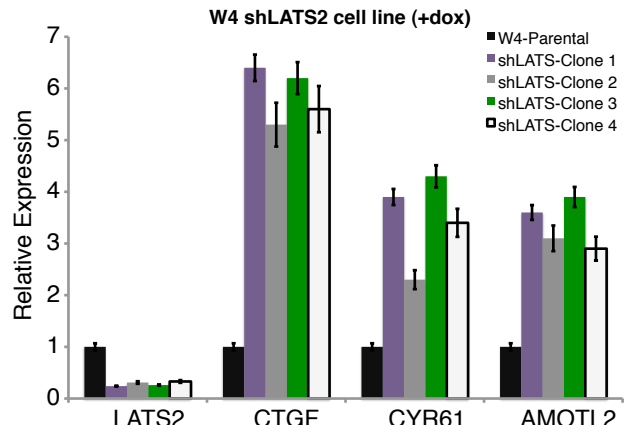
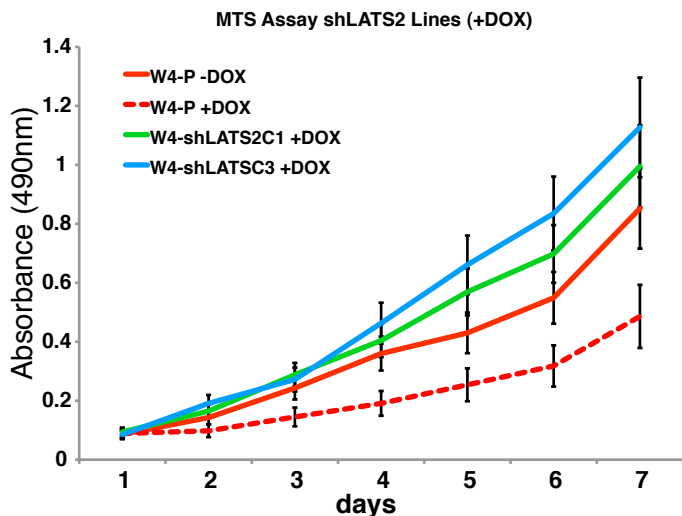
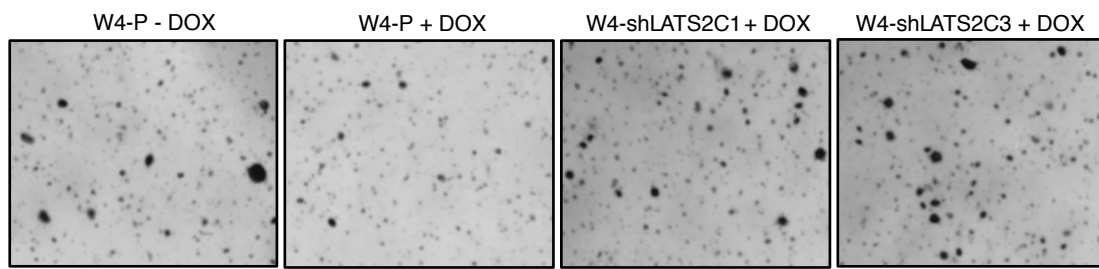
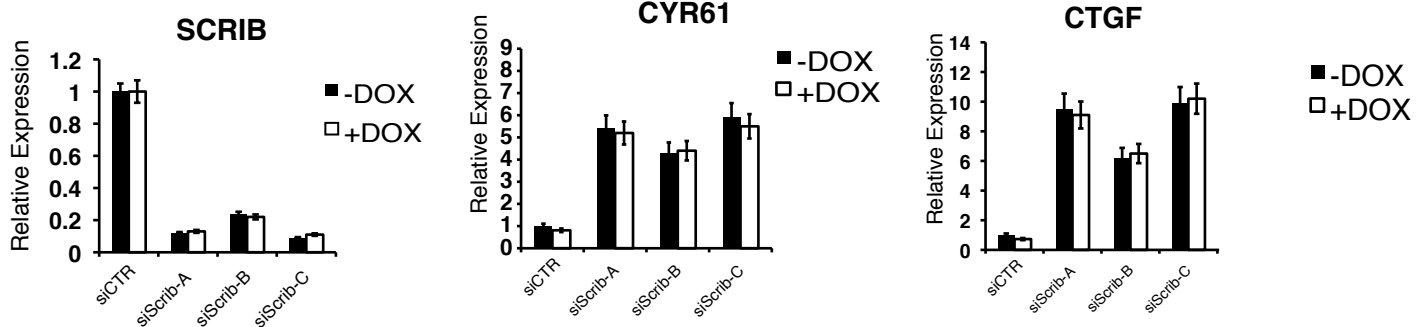
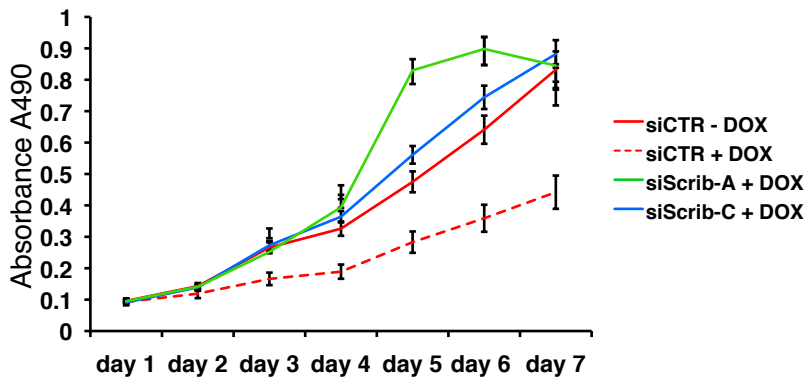
Hippo Signature

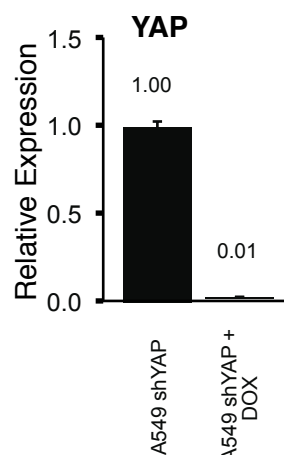
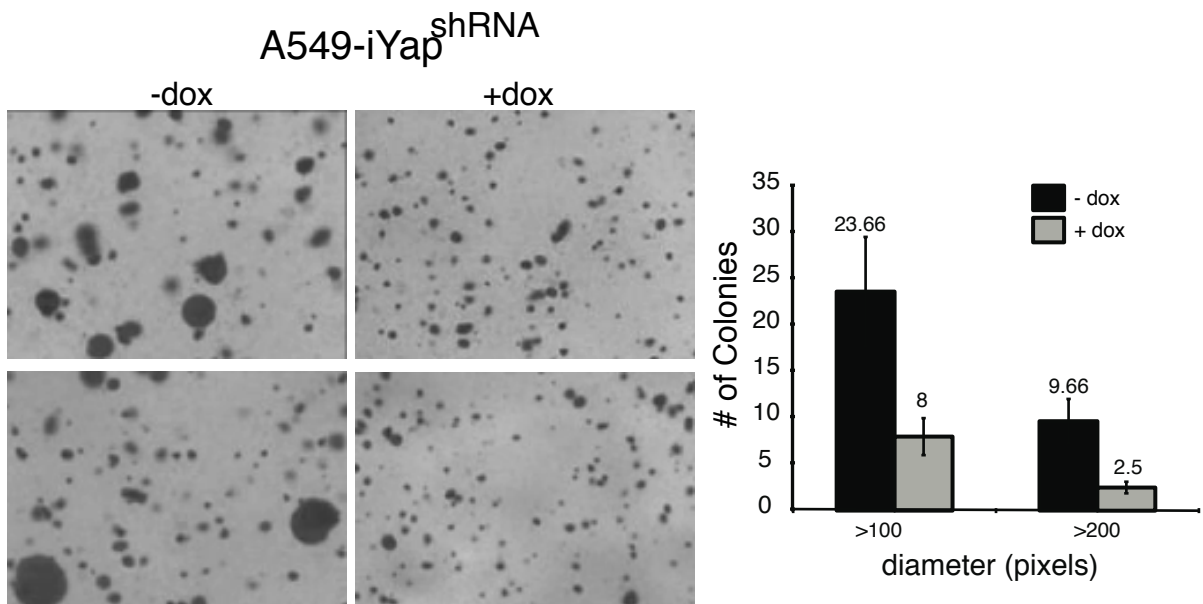
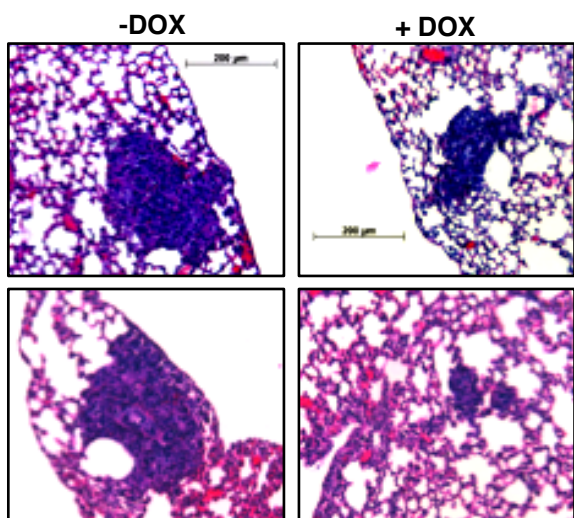
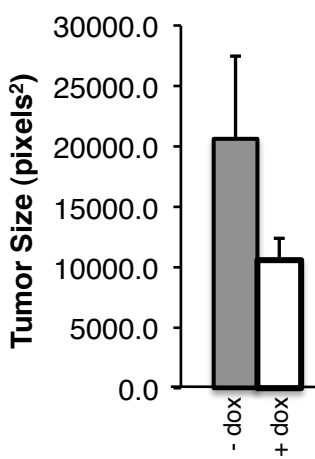
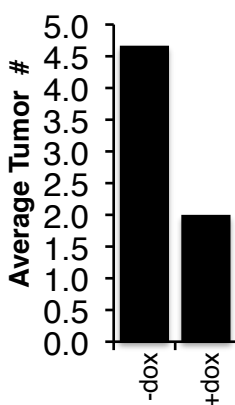
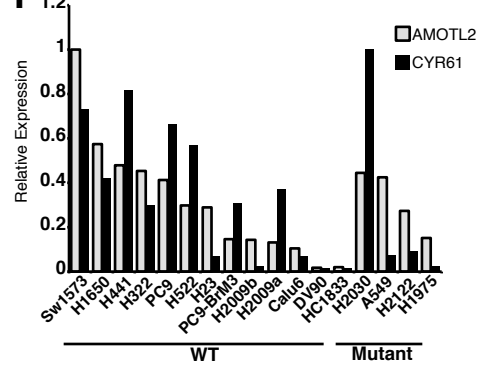
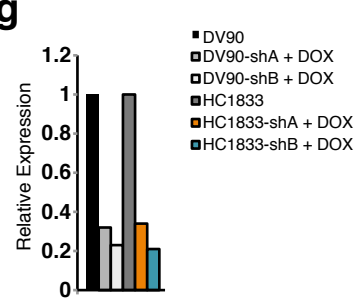
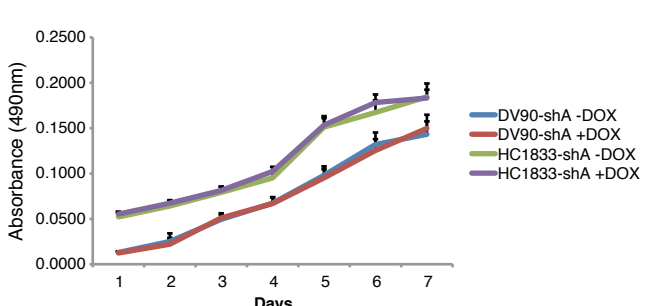
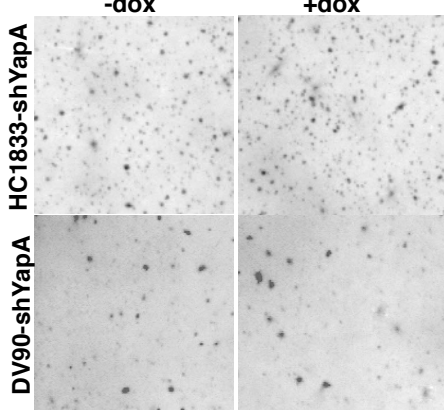
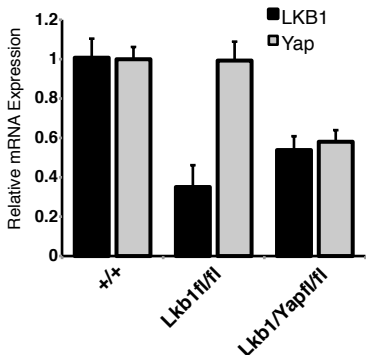
ABL2	MID1	FST	SLC16A6
ACAT2	MIR622	GADD45A	SLC2A3
ACLY	MYBL1	GADD45B	
ACSL1	MYOF	GCNT4	SLC43A3
ACSL4	NCF2	GDPD3	SLC48A1
ACSS2	NFKBIA	GGT5	SLC5A1
ADAMTS12	NID2	GPCPD1	SLC5A3
AMOTL2	NPPB	GPRC5A	SLC7A7
ANKRD1	NT5DC3	GPRC5B	SLC02A1
ANXA3	NT5E	HBEGF	SLIT2
AREG	NUAK2	HMGCS1	SNAPC1
AXL	OLFML3	HSPB8	SNORA75
BCAS1	OLR1	HSPC159	SNORD13P2
C6ORF155	OPN3	ICAM1	SNORD21
CALB2	P2RY8	IDI1	SNORD38A
CCL28	PCYT2	IFFO2	SNORD53
CCL5	PDCD1LG2	IFIT2	SNRPG
CD55	PDP2	IGFL1	SQLE
CDH2	PHLDA1	IL1A	STXBP1
CHST9	PLAU	IL1B	SYT14
CLDN1	PLAUR	IL32	TFPI2
CLDN4	PLK2	IL8	TGFA
CLMN	PLK3	INSIG1	TGFB2
COTL1	PRRG1	ITGA5	TGM2
COX6C	PSAT1	ITGBL1	THBS1
CPA4	PSG5	JPH1	TIMP2
CRYAB	PTPN14	KLK7	TLCD1
CTGF	RAB11FIP1	KPNA7	TMEM154
CTH	RAB3B	KRT18	TMEM171
CTNNAL1	RBM14		TMEM27
CYR61	RBMS2	KRT8	TNF
CYTH3	RGNEF	KRT81	TNFAIP3
DENND3	RIMKLB	LAMB1	TNFRSF9
DHCR7	RND3	LDLR	TNFSF18
EBP	SAA1	LIF	TSC2D2
ENC1	SAA2	LIPH	TUFT1
EPB41L2	SC4MOL	LMBRD2	UBD
ERRFI1	SCD	LOC100130876	UCA1
EXPH5	SCD5	LOC642947	UCP2
F3	SCML1	LOXL4	UGCG
FASN	SEMA7A	LPHN2	UPK1B
FDFT1	SERPINB10	LPIN1	UPP1
FDPS	SERPINB2	MACC1	VGLL1
FGFBP1	SHROOM3	MFAP5	WIP1
FLNA	SLC16A13	MICB	

FIGURE S9

a**b****FIGURE S10**

a**b****c****FIGURE S11**

a**b****c****d****e****FIGURE S12**

a**b****c****d****e****f****g****h****i****j****FIGURE S13**

Type of file: table

Label: Table S1, S2

Filename: 44560_0_supp_1865293_mkrpkf_Part2.pdf

	Average Fold	Average Z	Average Fold	Average Z	Average Fold	Average Z
	A	A	B	B	C	C
ABL2	6.436	2.687	-2.118	-1.539	10.604	3.044
AKAP8	5.383	3.866	4.630	4.773	-0.225	-0.591
EPHA7	1.207	0.383	4.225	2.293	5.818	3.923
GAK	4.859	3.441	5.511	3.680	9.522	2.478
LY6G5B	4.480	2.311	5.193	2.534	-0.212	-0.252
MAGI1	8.555	2.408	1.033	0.093	7.005	2.271
MAP2K7	8.211	2.264	4.943	2.179	1.349	1.771
MAP3K9	1.512	0.588	6.162	2.583	6.962	3.738
MAP4K4	1.374	1.055	6.210	2.273	4.227	2.318
MAP4K5	1.373	1.037	4.947	2.750	6.157	4.486
MAPKAPK5	5.889	2.719	4.900	3.940	-1.314	-1.233
MYLK2	1.267	1.288	8.309	3.501	8.857	3.332
NEK4	6.083	4.131	5.395	6.103	-1.787	-2.261
RIPK3	4.220	2.356	1.305	0.937	7.561	15.165
SGK1	4.830	2.241	4.540	5.059	1.769	2.134
STK10	1.486	1.853	4.528	2.315	4.717	3.651
STK11	4.772	2.122	6.578	12.887	1.346	0.787
STK33	4.093	2.032	-1.893	-0.985	3.614	5.926
TAOK1	1.593	2.661	4.930	5.693	4.297	6.484
TESK1	8.643	2.530	5.854	5.837	1.603	1.938
TRAF3IP3	7.915	2.325	4.635	7.653	0.134	0.397

TABLE S1

	Average Fold	Average Z	Average Fold	Average Z	Average Fold	Average Z
	A	A	B	B	C	C
MARK1	1.512	1.588	4.538	5.572	1.716	1.621
MARK3	2.143	1.171	2.301	1.340	1.503	1.855
MARK4	2.341	1.406	1.296	1.231	2.582	1.255
EPHA4	2.318	1.489	-0.394	-0.762	1.709	1.597
EPHA5	1.395	2.395	2.610	2.297	1.580	1.748
EPHA7	1.207	0.383	4.225	2.293	5.818	3.923
EPHA8	4.199	0.588	1.517	1.027	1.517	2.099

TABLE S2